Journal of Applied Mechanics and Technical Physics, Vol. 50, No. 1, pp. 163–169, 2009

DEFORMATION AND FRACTURE OF A SPHEROPLAST UNDER LOW-CYCLE LOADING AT VARIOUS TEMPERATURES

E. V. Karpov

UDC 539.0

This paper gives the results of an experimental study of the deformation and fracture of a spheroplast under uniaxial low-cycle loading (compression and unloading) at a temperature $T = 25$ *and* 100°C. *Various mechanisms of damage accumulation at various temperatures and degrees of damage to the material are studied. The experimental results are compared with the well-known dependences taking into account damage accumulation for metals. It is established that the basic propositions of these theories are suitable for the low-cycle fracture of spheroplast — a ductile material of complex structure.*

Key words: *spheroplast, composite, cyclic loading, low-cycle fatigue, damage accumulation.*

Introduction. At present, there is a large number of the papers dealing with the low-cycle fatigue of metals and alloys. Coffin derived the equation of low-cycle strength [1]

$$\varepsilon_p N^{1/2} = c \tag{1}$$

(ε_p is the plastic strain increment in one cycle, N is the number of cycles before fracture, and c is a material constant). Manson and Martin proposed more general dependences [2, 3]:

$$\varepsilon_p N^k = c \tag{2}$$

(k is a constant which, for different materials, take values of 0.2 to 1.0 [4]). From (1) and (2), it follows that, for cyclic elastoplastic deformation, the operating life of metals and alloys depends only on the accumulated plastic strain and does not depend on the type of stress state. Similar trends are known for the creep of metallic structural materials. According to the energetic version of creep theory [5, 6], each material is characterized by a constant value of the critical dissipated energy at which creep ends with fracture regardless of the type of stress state and the stress value. This hypothesis is supported by the results of experiments with samples of St. 45 steel and various titanium and aluminum alloys. The dissipated energy is taken to be a measure of the damage to the material.

The present paper gives the results of experimental studies of the deformation and fracture of ÉDS-7A spheroplast under low-loading cycle at a temperature $T = 25$ and 100°C. Spheroplast is a material whose mechanical properties differ substantially from the mechanical properties of metals. Spheroplast, which has a complex structure, consists of components reacting differently to temperature variation and loading and contains a large number of microconcentrators. However, the studies show that, with all differences between the mechanical properties of spheroplasts and metals, the behavior of the low-cycle fatigue of spheroplast is similar to that of metals.

1. Material and Conditions of Experiments. ÉDS-7A spheroplast is a composite porous reinforced material consisting of epoxy-diane resin filled with glass microspheres. The diameter of the microspheres can reach $120 \cdot 10^{-6}$ m, but the diameter of most of them is $20 \cdot 10^{-6}$ to $70 \cdot 10^{-6}$ m, and the thickness of their walls is approximately 10^{-6} m and does not depend on the sizes of the spheres. The volume fraction of spheres in the material is about 60%. At $T = 25$°C, Young's modulus is 2060 MPa, Poisson' ratio is $\nu = 0.3$, and the density is 700 kg/m^3. Figure 1 shows a photograph of the microstructure of the material taken with a LEO-420 scanning electronic microscope.

Lavrent'ev Institute of Hydrodynamics, Siberian Division, Russian Academy of Sciences, Novosibirsk 630090; evkarpov@mail.ru. Translated from Prikladnaya Mekhanika i Tekhnicheskaya Fizika, Vol. 50, No. 1, pp. 197–204, January–February, 2009. Original article submitted November 28, 2007; revision submitted December 20, 2007.

0021-8944/09/5001-0163

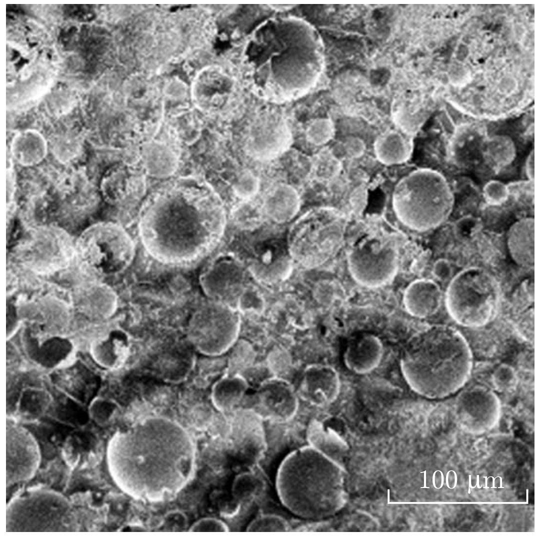

Fig. 1. Microstructure of spheroplast.

During the tests, cylindrical samples were subjected to cyclic uniaxial loading at $T = 25$ and 100°C. The choice of the value $T = 100$°C is due to the fact that heating to this temperature does not result in irreversible changes in the material but, as it is reached, the nature of the fracture of the spheroplast changes and its compression strength sharply decreases (at lower temperatures, heating leads to an increase in the strength). The experiments were performed on a Zwick/Roell Z100 TC-FR100TL.A4K test machine. Pulsed loading (repeated alternation of compression and unloading) was carried out by moving a mobile traverse at a constant velocity which provided a strain rate of $1.5 \cdot 10^{-3}$ sec^{-1} Strain was measured by a traverse-displacement transducer (the rigidity of this material allows high-accuracy strain measurements using this method), and the applied force was measured by a built-in strain gauge. During unloading of the sample, the measurements were not included in the database because of the limited capabilities of the equipment configuration.

It should be noted that, for uniaxial compression, the diagram $\sigma(\varepsilon)$ of the spheroplast is similar to the diagram $\sigma(\varepsilon)$ of an elastoplastic material. However, in the linear region of the diagram $\sigma(\varepsilon)$, the deformation can only conditionally be considered elastic since each loading leads to an increase in the residual strain, which, in a certain number of cycles (of order of 10^3) can lead to fracture of the material. The curvature of the diagram with increasing load is due not to plasticity but to the accumulation of a large number of local ductile fractures of the structure (cracks in the matrix near the microspheres, which play the role of stress concentrators, and fractures of the microspheres).

In the case of metals, low-cycle fatigue is meant for elastoplastic cyclic strain. In the case of spheroplast, any load comparable to the strength limit results in irreversible deformation of the material even if the yield point [calculated by the diagram $\sigma(\varepsilon)$ using the conventional method] is not exceeded. Therefore, below, instead of plastic strain, we consider irreversible compression strain ε_n accumulated during cyclic deformation.

2. Cyclic Loading at a Temperature $T = 25$°C. At $T = 25$°C, the samples were subjected to nonstationary pulsed loading, in which the loading cycles were united in groups with a constant value of the maximum stress $\sigma_{\max}$. Below, this group of cycles is called the step of nonstationary cyclic loading. Transition from one loading step to the next was performed by increasing the value of $\sigma_{\max}$ by 2 MPa. Two loading modes were used. In the first mode, with 20 cycles in one step, the number of cycles before fracture was $N = 282$. In the second mode, with 50 cycles in one step, $N = 450$. The main difference between these modes is that the accumulation of the same residual strain requires a larger of cycles in the second mode than in the first mode. Experimental diagrams $\sigma(\varepsilon)$ for the first and second modes are presented in Figs. 2 and 3, respectively. Because of the large number of cycles, Fig. 2 gives each third curve, and Fig. 3 each fifth curve.

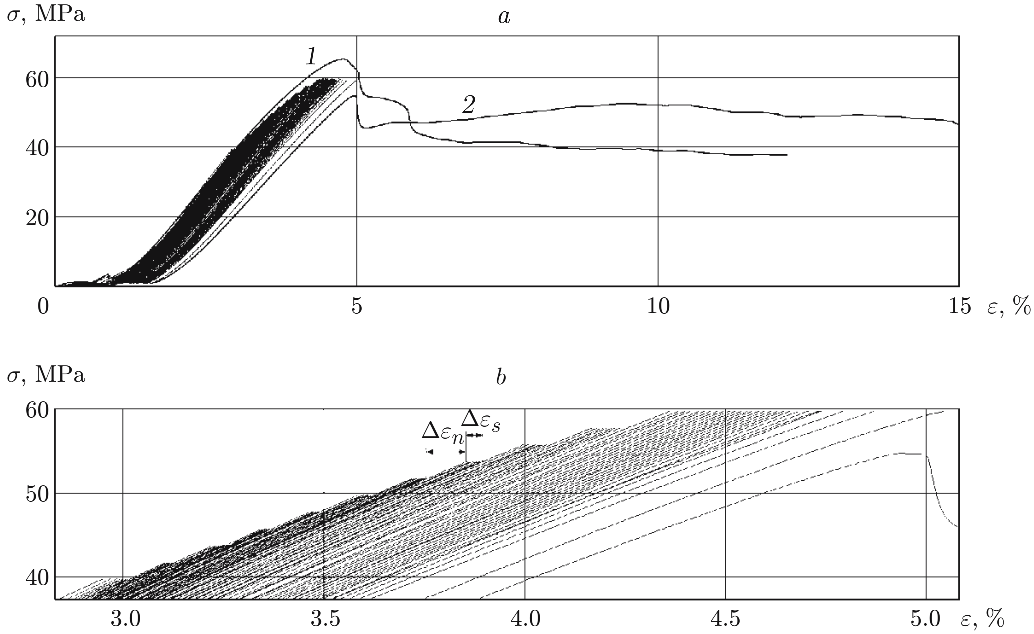

Fig. 2. Diagrams $\sigma(\varepsilon)$ in the case of cyclic compression at $T = 25°$C in the first loading mode: (a) single-loading curve (1) and curve for the last loading cycle (2); (b) determination of the quantities $\Delta\varepsilon_n$ and $\Delta\varepsilon_s$.

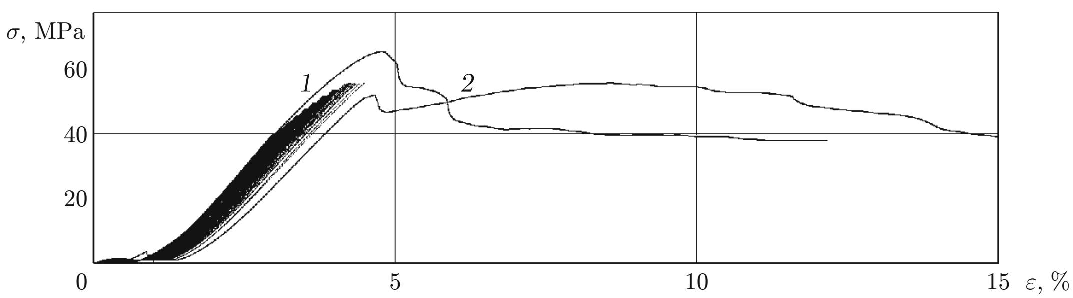

Fig. 3. Diagrams $\sigma(\varepsilon)$ in the case of cyclic compression at $T = 25°$C in the second loading mode: single loading curve (1) and curve for the last loading cycle (2).

The relative compression strain and the irreversible strain accumulated for i of cycles are equal, respectively, to

$$\varepsilon = \frac{h_0 - h}{h_0}, \qquad \varepsilon_n^i = \frac{h_0 - h_i}{h_0}$$

(h_0 is the height of the sample before the beginning of the experiment, h is the current height of the sample, and h_i is the height of the sample after the completion of the ith cycle). The horizontal region of the ith curve lying on the abscissa corresponds to the irreversible strain ε_n^{i-1}.

Let $\varepsilon_{\max}^i$ be the maximum strain for the ith cycle. Then, the quantity $\Delta\varepsilon_c^i = \varepsilon_{\max}^i - \varepsilon_{\max}^{i-1}$ will be called the additional strain of the ith cycle. In the case of loading at room temperature, $\Delta\varepsilon_c^i = \varepsilon_n^i - \varepsilon_n^{i-1}$. The quantity $\Delta\varepsilon_s$, which is equal to the sum of all $\Delta\varepsilon_c^i$ in one loading step, will be called the additional strain in the step.

In Fig. 2b, it is evident that, during the experiment, the value of $\Delta\varepsilon_s$ first decreases from step to step to a certain value and then begins to increase. In the first step, stabilization of damage accumulation occurs, which is manifested in a nonlinear decrease in the value of $\Delta\varepsilon_c^i$ depending on the number of loading cycles. In all steps beginning from the second, the value of $\Delta\varepsilon_c^i$ is almost identical for all cycles of the same step. Obviously, stabilization of damage accumulation continues after the first step, This is manifested in a decrease in the value of $\Delta\varepsilon_s$; in this case, the decrease in $\Delta\varepsilon_c^i$ is so insignificant that it is difficult to detect within one step. The substantial nonlinearity

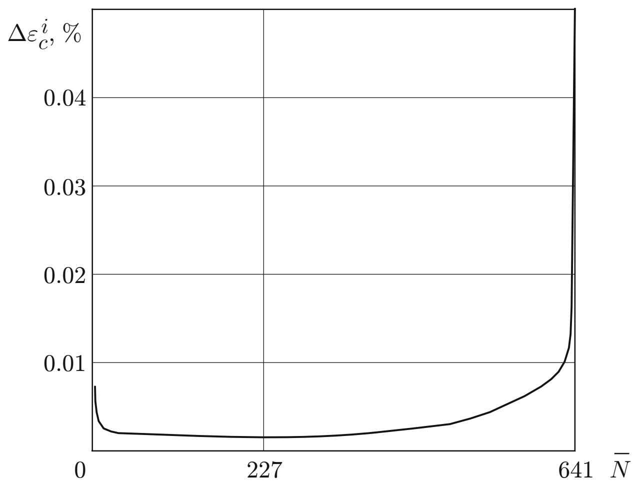

Fig. 4. Residual strain increment $\Delta\varepsilon_c^i$ in one cycle versus the number of cycles $\bar{N}$.

of $\Delta\varepsilon_c^i$ in the first step can be attributed to gradual fracture of those structural elements whose size exceeds the average characteristic size. After fracture of such elements (for example, microspheres with diameter much greater than the average value), the material becomes more homogeneous, resulting in stabilization of the residual-strain accumulation. Similar trends in the accumulation of irreversible strain are observed for the second loading mode. Stabilization of damage accumulation in both loading modes continues until the value of the accumulated residual strain ε_n approaches the value $\varepsilon_n^* = 0.45\%$, after which $\Delta\varepsilon_s$ and $\Delta\varepsilon_c^i$ begin to increase from step to step. In the first loading mode, the minimum value of $\Delta\varepsilon_c^i$ is about 0.002%, and the maximum value reached in the next-to-last 10th step is 0.005%. The last loading step differs from the previous steps in that it involves the process inverse to the stabilization of damage accumulation observed earlier: the value of $\Delta\varepsilon_c^i$ increases nonlinearly from cycle to cycle, which ultimately leads to fracture of the sample under a load smaller than the value of $\sigma_{\max}$ in this step. After the beginning of growth in the value of $\Delta\varepsilon_c^i$, the value of $\sigma_{\max}$ did not increase; therefore, the last loading step, which continued up to the fracture of the sample, included 82 cycles (see Fig. 2).

A comparison of the experimental results for the first and second loading modes shows that the change in the value of $\Delta\varepsilon^i$ with transition from one loading step to another is due not so much to an increase in the maximum stress $\sigma_{\max}$, but rather to an increase in the irreversible strain ε_n with increasing $\sigma_{\max}$. In both modes with close strains, similar processes occur, although these strains correspond to different stresses.

Since the changes $\Delta\varepsilon_c^i$ from step to step are small compared to the value of the residual strain $\Delta\varepsilon_s$ accumulated in these steps, the residual-strain increments $\Delta\varepsilon_n$ due to an increase in the maximum stress during transition to the next step will be treated as the strain $\Delta\varepsilon_s$ accumulated in the additional steps with a constant value of $\Delta\varepsilon_c^i$ as the residual strain. This value will be set equal to the mean arithmetic of the corresponding values for the previous and subsequent steps. We set the number of cycles in each such step equal to the integer part of $\Delta\varepsilon_n/\Delta\varepsilon_c^i$. Representing the loading process as a continuous sequence of cycles without jumps of the strain in transition from step to step, we obtain the dependence of $\Delta\varepsilon_c^i$ on the number of cycles presented in Fig. 4. This dependence is constructed for the first loading mode; the dependence for the second mode is similar. Instead of the number of the loading cycles implemented N, we use the quantity $\bar{N}$ obtained by the addition of the total number of cycles in the additional steps to N. In Fig. 4, the value $\bar{N} = 227$ for the first mode corresponds to the accumulated residual strain $\varepsilon_n^* = 0.45\%$ at which the decrease in the value of $\Delta\varepsilon_s$ in both modes is replaced by its increase. If the constant c in the Coffin formula is determined as the irreversible strain obtained before the beginning of macrofracture under single loading, the dependence between $\Delta\varepsilon_c^i$ and the limiting strain before the beginning of macroscopic fracture can be described by the formula

$$\Delta\varepsilon_c^{\min}(\bar{N}_1^{k_1} + \bar{N}_2^{k_2}) = c. \tag{3}$$

Here $\Delta\varepsilon_c^{\min}$ is the value of $\Delta\varepsilon_c^i$ which is minimal for the given loading mode; $\bar{N}_1$ is the number of cycles before the beginning of growth in $\Delta\varepsilon_s$ begins; $\bar{N}_2 = \bar{N} - \bar{N}_1$; k_1 and k_2 are material constants (for the first loading mode, $k_1 = 1.05$ and $k_2 = 1.15$, for the second mode, $k_1 = 1.03$ and $k_2 = 1.15$). The values of the constants obtained in

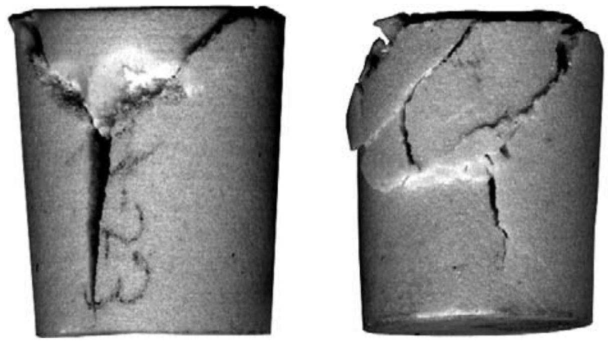

Fig. 5. Fracture of samples in single (a) and low-cycle (b) loading.

these experiments k_1 and k_2 are approximate. To determine them more exactly and to determine the constant ε_n^* required to calculate $\bar{N}_1$ and $\bar{N}_2$, it is necessary to perform additional series of experiments with stationary low-cycle loading (with a constant value of $\sigma_{\max}$). However, the possibility of determining these constants indicates that low-cycle fatigue processes in the spheroplast obey the regularities close to those established for metals and alloys.

In the case of loading at room temperature, Young's modulus changes significantly only in a few cycles before the beginning of macroscopic fracture when the value of $\Delta\varepsilon_c^i$ begins to increase rapidly (see Fig. 4). During the experiment (except in the last few cycles), the deviation of Young's modulus from its initial value does not exceed 1.5%.

Fracture of the sample can occur at loads much smaller than the stress limit of the material under single loading, but, after the strain drop due to the formation of a macrocrack during the further compression of the sample, the stress increases. As a result, before the final loss of the load-bearing capacity, the sample subjected to cyclic loading withstands much larger strains than the sample fractured by single loading (see Fig. 2a and Fig. 3). In this case, the maximum stress reached in the sample after the formation of macrocracks can be higher than the stress at which macrofracture (see Fig. 3) began. This may be due to a more uniform distribution of damage in the material (Fig. 5).

From Figs. 2 and 3, it follows that, in the second loading mode, where a larger number of cycles is required to attain the same value of the accumulated residual strain as in the first mode, fracture occurs not only at a smaller load but also for a smaller value of the accumulated residual strain. The latter may be due to the fact that, in the second mode (see Fig. 3), the number of cycles before fracture was 1.5 times larger than that in the first mode (see Fig. 2). The fact is that not all fractures of the structure resulting from the compression of the samples can cause residual longitudinal deformation. Fractures that may not cause residual deformation are microcracks characteristic of porous media that arise in the binder near spherical voids and directed along the loading axis. Without influencing an increase in the residual compression strain, these fractures are, nevertheless, accumulated from cycle to cycle, increasing the damage to the material, which, with increasing number of cycles, can lead to a reduction in the maximum fracture strain of the sample.

3. Low-Cycle Loading at a Temperature $T = 100°$C. Figure 6 gives experimental diagrams $\sigma(\varepsilon)$ obtained in the case of low-cycle loading at a temperature $T = 100°$C. A total of 63 cycles were performed.

In the beginning of loading of spheroplast samples at stresses much smaller than the strength, the diagram $\sigma(\varepsilon)$ over the entire temperature range has a portion (in Fig. 6, it is shown by dashed curves) which separates the linear portions of the diagram. During cyclic loading in this portion, the curves of the diagram $\sigma(\varepsilon)$ retain their shape (which is individual for each sample), and, hence, it is neither an yield area nor the result of local fracture of the material during the initial stress redistribution in the sample. Obviously, the presence of this portion in the diagram is due to a reversible process.

At $T = 100°$C, the process of damage accumulations in the material differs from that at room temperature. Residual compression strains are not accumulated in the sample, and the increase in the strain corresponding to the maximum stress $\sigma_{\max}$ is due to a decrease in Young's modulus of the material [if it is calculated by the linear region of the diagram $\sigma(\varepsilon)$ following the portion shown by dashed lines in Fig. 6, for example, in the interval from 4

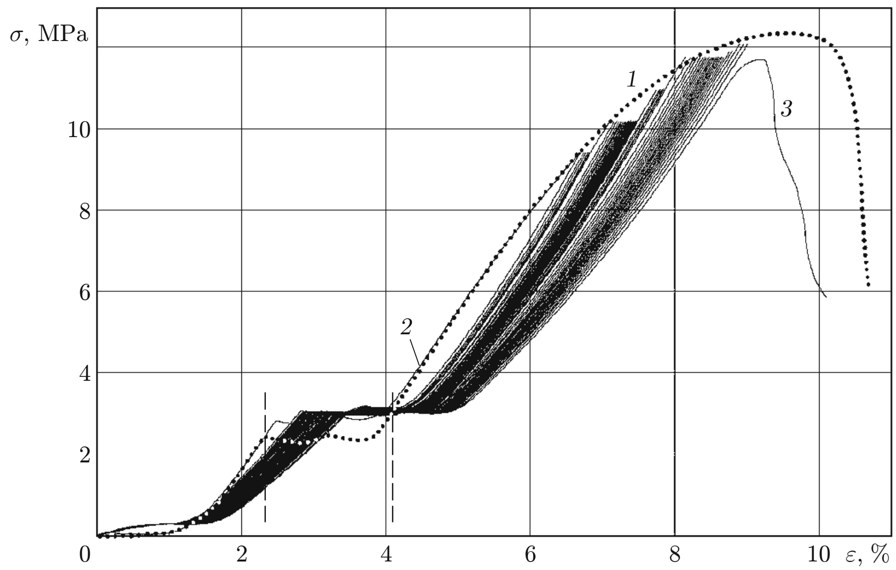

Fig. 6. Diagrams $\sigma(\varepsilon)$ in the case of cyclic compression at $T = 100^\circ$C: curve of single loading before fracture (1), curve in the first step of cyclic loading (2), and curve in the last step of cyclic loading (3).

to 9 MPa]. As a result, in the last cycle, which ends with fracture, Young's modulus is 12% smaller than the initial value equal to 250 MPa. This change in the properties is explained by an increase (at a high temperature) in the deformation strength of the binder, accompanied by a considerable reduction in its rigidity; as a result, most of the load falls on the microspheres. In this case, fracture of microspheres can occur without damage to the matrix; as a result, Young's modulus of the sample decreases without accumulation of residual compression strains. Reduction in the rigidity of the material may also be caused by the accumulation of cracks in the binder that are directed along the loading axis (see Sec. 2).

At $T = 100^\circ$C (unlike at room temperature), damage accumulation is substantially nonlinear. For each value of the maximum stress $\sigma_{\max}$, the value of $\Delta\varepsilon_c^i$ decreases from cycle to cycle (the refining of loading curves in Fig. 6), i.e., stabilization of damage accumulation occurs. After the value of $\Delta\varepsilon_c^i$ reaches a certain limiting value, the Young's modulus ceases to decrease monotonically and only fluctuates in the vicinity of the value reached. At loads close to the critical value in the case of single loading, the value of $\Delta\varepsilon_c^i$ does not approach zero, as it does at smaller loads, but decreases to a certain value accessible to measurements and then remains constant. The exception is the last few cycles, in which $\Delta\varepsilon_c^i$ increases until the onset of fracture. Unlike in the case where loading occurs at room temperature, the load bearing capacity after macrocrack formation is not retained.

4. Conclusions. The results of the experiments show that the low-cycle fatigue of spheroplast is similar in behavior to that of metals and alloys. At least, for spheroplast at room temperature, it is possible to obtain an equation of operating life similar to the Coffin equation.

According to various theories, damage accumulation can be a linear [6] or nonlinear [1] process. In the case of spheroplast, damage accumulation for the same material follows both linear and nonlinear laws, depending on the temperature at which cyclic loading occurs and depending on the degree of damage to the material.

At a temperature higher than room temperature that does not cause irreversible changes of the material, the mechanism of damage accumulations changes in low-cycle fatigue. At room temperature, an increase in the degree of damage is manifested in an increase in the residual compression strain without significant changes in the rigidity of the material, whereas at a temperature $T = 100^\circ$C, Young's modulus of the material (by the moment of fracture, Young's modulus is 88% of the initial value) decreases without increment in the residual compression strain.

This work was supported by Integration project of the Department of Power Engineering, Machine Building, Mechanics, and Control Processes of the Russian Academy of Sciences (Grant No. 4.12.2) and the Russian Foundation for Basic Research (Grant No. 05-01-00728).

REFERENCES

1. L. F. Coffin and Jr. Schenectady, "Study of the effects of cyclic thermal stresses on a ductile metal," *Trans. ASME*, **76**, No. 6, 931–950 (1954).
2. S. S. Manson, *Thermal Stress and Low-Cycle Fatigue*, McGraw-Hill, New York (1966).
3. D. E. Martin, "An energy criterion for low-cycle fatigue, *Trans. ASME, Ser. D*, Dec. 565–571 (1961).
4. V. T. Troshchenko, *Fatigue and Inelasticity of Metals* [in Russian], Naukova Dumka, Kiev (1971).
5. O. V. Sosnin, B. F. Gorev, and A. F. Nikitenko, *Energetic Version of Creep Theory* [in Russian], Inst. of Hydrodynamics, Sib. Div., Novosibirsk (1986).
6. A. F. Nikitenko, *Creep and Long Life of Metallic Materials* [in Russian], Novosibirsk State University of Architecture and Civil Engineering, Novosibirsk (1997).